Contrasting the 1997/1998 and 2015/2016 El Niño Episodes Using Satellite Radar Altimetry and Sea Surface Temperature Data

Senior Research Thesis

Presented in partial fulfillment of the requirements for graduation

With research distinction in Earth Science in the undergraduate

colleges of The Ohio State University

By

Taylor M. Allen

May 2016

Dr. C. K. Shum, Advisor
School of Earth Sciences

TABLE OF CONTENTS

Abstract

The El Niño-Southern Oscillation (ENSO) is a topic of increasing scientific and public interest due to the air-sea interaction processes that cause the westerly winds to weaken in the equatorial Pacific (National Geographic Society, 2016). Each El Niño event is different than any other and shows large ranges in their intensities in the form of mean sea level (MSLA) and sea surface temperature (SSTA) anomalies. At this point in history, the El Niño event of 1997–98 has been categorized as the largest on record. However, recent scientific discoveries have suggested that the 2015–16 event has many similar characteristics of 1997–98. This study focuses on contrasting the two events using satellite altimeter data from four satellite missions and sea surface temperature data to qualitatively and statistically address this inquiry. Our analysis concludes that while both are similar in intensity and magnitude, the 1997–98 event has a greater intensity for both SSTA and MSLA up to February 2016. However, the 2015–16 El Niño has a wider spatial reach in mean sea level anomalies across the western Pacific. It seems to have been spanning longer, for almost three years and still going, than the 1997–98 El Niño. This study requires more processed satellite data for the rest of 2016 in order to get a more complete representation of the 2015–16 El Niño, for a final comparison of the two El Niño's. Though, the acquisition of these data would still require further research into local weather patterns at different locations to get a better understanding of how the episodes progress and which is truly the strongest on record.

Acknowledgements

I would like to thank Dr. C.K. Shum, Dr. Junkun Wan, and Ms. Ting-Yi Yang of The Ohio State University School of Earth Sciences for their extensive effort in shaping my research and their continued support to help with the data processing utilized in this thesis. Without their support and guidance, this thesis would have never been a possibility. My research and their expertise are also due in large part supported by a grant from the National Science Foundation (No. ICER-1342644). I would also like to extend my thanks to National Aeronautics and Space Administration (NASA), National Oceanic and Atmospheric Administration, Aviso^{+} (CNES data) satellite data and graphs, and the Permanent Service for Mean Sea Level, for providing me with the multiple mission radar altimeter, tide gauge, and sea surface temperature data, and to Professor Chungyen Kuo of National Cheng Kung University in Taiwan for his help in near-real altimeter data processing, and Dr. Xiaochun Wang of NASA Jet Propulsion Laboratory for his advice on scientific questions regarding El Niño. I would also like to show my appreciation to Dr. Anne Carey who encouraged me to apply for research distinction and promptly assuaged my panic attack that followed.

I would, likewise, wish to thank those who played a more silent role in my actual research and thesis, but were just as important to me. My friends who've supported me and kept me motivated even as senioritis often reared its ugly head. They always knew that I did not mean the things I said while hopped-up on caffeine and sleep-deprived; especially, Bridgette and Michaela, whom are the two best friends I could have ever hoped for. Finally, I would like thank the people who helped produce the person I am today: my family. This journey, while rewarding has not been easy. But, their love and unyielding support has gotten me through some very trying times. I appreciate all they have done and would like to dedicate this thesis to them. Thank you.

List of Figures

Background And Study Objectives

In the context of weather and climate, the El Niño Southern Oscillation or ENSO cycle is a topic of scientific interest with its considerable impact on societies. The term El Niño and its counter phase, La Niña, originate from air-sea interactions causing reoccurring fluctuations in the temperatures between the ocean and the atmosphere, and the associated sea level change (Monastersky, 2016). El Niño refers to the warm phase of ENSO and La Niña corresponding with the cold phase. These temperature oscillations only transpire in the Equatorial Pacific, and typically last from nine to twelve months (National Geographic Society, 2016). El Niño (and La Niña) often exhibit irregular frequency anywhere between every two to seven years, where El Niño is the more frequent of the two phenomena (National Geographic Society, 2016). Focusing on the El Niño effects where there is a large-scale atmosphere climate interaction, most of the noticeable affects are likely to develop over North America during its winter seasons. During which this land mass experiences warmer average temperatures over the northern United States, but wetter and slightly colder conditions near the U.S. Gulf Coast and in South America, and other large weather pattern changes over other parts of the world, affecting society and human beings (Ying et al., 2016).

In the ocean, conditions during an El Niño event, trade winds blowing west weaken near the Pacific Equator thus changing the water direction eastward from the western Pacific to the north coast of South America. This change in direction disturbs the upwelling, atmospheric circulation and convection patterns that occur naturally along the equator because of a warmer layer of ocean water occupy the space where it was once colder (National Geographic Society, 2016). These disruptions cause catastrophic damage to continental economics, develop increased precipitation contributing to coastal flooding and erosion, and short-term climate variations (Monastersky, 2016). Historically, El Niño events have been evaluated via networks of moored scientific buoys or *in-situ* instruments in the equatorial Pacific Ocean. These instruments most often are only able to measure

temperature profiles within the upper ocean. The buoys record measurements made with respect to the Earth's geoid at a fixed level on land and detect the global sea level rate and any vertical land motion (Trococoli et al., 2008). The instruments, like the eXpendable BathyThermographs (XBTs), and more recently the more densely sampled Argo arrays (http://argo.ucsd.edu), record those data and transmit them via wireless communications to the data center located at the University of California at San Diego. These observations can also be used to provide information on the ocean's subsurface dynamic features, producing the so-called steric sea level change over the last few decades.

However, since the early 1990's, with the beginning of satellite radar altimeters and the advent of satellite oceanography, the *in-situ* data derived steric sea level have been used, together with satellite altimetry sea level measurement to estimate the mass variation component of the sea levels (Troccoli et al., 2008). Satellites in oceanography has made it possible for researchers remotely to measure the sea surface temperature (SST), sea surface height (SSH), and even, sea surface salinity (SSS) (Troccoli et al., 2008). The satellite sea surface temperature measurements are obtained by the so-called multi-spectral radiometers, launched by NOAA, with multi-decadal observational records. Here we obtained the SST data by downloading data from their web site: http://www.ospo.noaa.gov/Products/ocean/sst/anomaly.

The process of remote measurements from satellite altimetry data is constructed by altimeters emitting signals towards Earth from the nadir of the satellites. The satellites then receive the echo from the sea surface after its reflection and record the travel time of said radar with a very precise (accurate to microseconds or better) clock (Troccoli et al., 2008). The range or distance of the radar measurements can then be used to compute the instantaneous sea surface height as a function of time, if the orbital height of the satellite is accurately known or computed. Since the Geosat satellite radar altimeter mission in the mid 1980's, there have been 11 more missions carrying

radar altimeters launched which orbited or are currently orbiting the Earth (Troccoli et al., 2008). For the purpose of this study, processed combined altimetry sea surface height data were taken from the NASA, CNES (French Space Agency) and European Space Agency (ESA) satellite altimetry missions, TOPEX/Poseidon, Jason-1, Jason-2, and Envisat satellites, supplied by CNES, via the AVISO+ (Archiving, Validation and Interpretation of Satellite Oceanographic Data, (http://www.aviso.altimetry.fr) Data Center.

Satellites are unique as they measure continuous sea level topography over a large spatial area, instead of stationary tide gauges. That data are then transmitted back to Earth. That data from the aforementioned satellites are the basis of this study that addresses the following objectives:

- Statistically address the accuracy of satellite SSH data compared to that of the direct-measurement tide gauges, to verify that we could study El Niño from space using the data,
- Qualitatively contrast the 1997/1998 El Niño episode, which is the largest event on record, with the current episode of 2015/2016, which is as large if not larger, with a combination of sea surface temperature and sea surface height data from multiple satellite missions
- Examine the evolutions of the two El Niño episodes via the observed parameters of SST and SSH or mean sea level (MSL) anomalies, and to study their amplitudes and correlations in the Western and the Eastern Pacific Oceans, to assess whether the 2015/2016 El Niño is comparable to the 1997/1998 El Niño

Study Region

The study area of this thesis is conducted in the equatorial Pacific Ocean. The altimetry data were taken from TOPEX/Poseidon, Jason-1, Jason-2, and Envisat satellite data centralized between 30°N and 30°S, with the largest focus on the equatorial region of the Pacific Ocean. The tide gauge data were extracted from Santa Cruz and Baltra-B of the Galápagos Islands from the Permanent Service of Mean Sea Level in the UK (http://www.psmsl.org). These islands are located

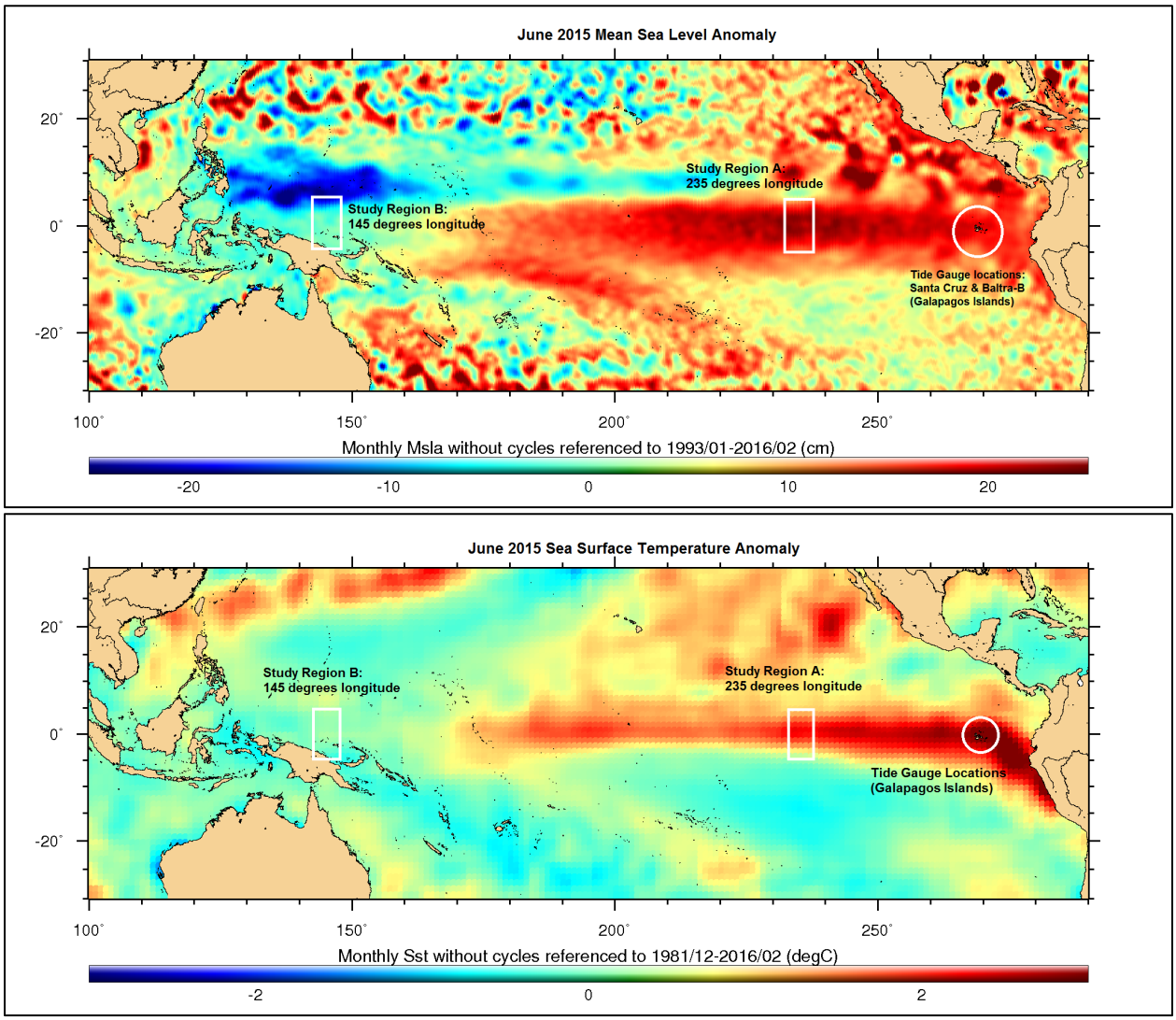

Fig. 1: Study Region depicting Pacific Ocean between 30°N and 30°S, with an example of the altimetry mean sea level anomaly map (**top**), and the sea surface temperature anomaly (**bottom**) averaged over June, 2015. White circular region is highlighting Galápagos Islands where both Santa Cruz and Baltra-B tide gauges locate. White boxes highlight two study regions where data were averaged for longitude time plots in the Western and Eastern Pacific, to examine the amplitudes and the correlations of the 1997/1998 and the 2015/2016 El Niños.

approximately 1,357 kilometers west of the coast of Ecuador in South America. Two Study Regions lie along the equator and used for longitude time plots. Region A is centered over 225° and Region B is centered over 140°. The regions extend 2.5° degrees to the east and the west and 5° north and south of the equator (**Fig. 1**).

Due to the influence of warmer water currents from the west and south, the Galápagos archipelago experiences dry and moderate climate, and is considered a subtropical group of islands (Manzello et al., 2014). During El Niño, trade winds slow in the central and western Pacific causing the warmest water to move east. This creates an unusual amount of precipitation over and warmth within the Pacific Ocean.

METHODS

The 1997/1998 El Niño episode is the largest event on record, the current 2015/2016 El Niño episode is still ongoing, and there is evidence that it is as large if not larger. To contrast these two El Niño events, it is necessary to first decide how long the time span will be between the different years. Data from January 1994 to December 1998 and January 2012 to February 2016 were considered, and the data used are satellite observed sea surface temperature (SSTA) and mean sea level anomalies (MSLA) for the explicit purpose of the comparison study. Anomaly is defined as the SST or MSL time series referenced to averaged quantities over the Pacific Ocean (Troccoli et al., 2008). Here it is adopted that the reference data span is January 1993–February 2016, and December 1981–February 2016, respectively for SSTA and for MSLA. Realistically, the Pacific Ocean was not under El Niño conditions at the beginning of each time frame. Using 1994 and 2012 data for plotting purposes allows us to establish a baseline of El Niño conditions between each year.

Tide Gauge Data vs. Satellite Altimeter MSLA Data

To test the accuracy of these satellites, tide gauge data from the Galápagos Islands were compared to the raw data from TOPEX/Poseidon and Jason-1 satellites. I wrote and utilized the Matlab code [Appendix A], that used both the raw sea level data from the Santa Cruz and Baltra-B tide gauges [raw data supplied by NOAA] with that of raw sea level data from the aforementioned satellites. Jason-1 sea level satellite data were included in the time series plots but the tide gauge data we have are only available until 2008. The plots from both locations along with the altimetry data were compared and the Pearson correlation coefficient was found by Matlab using this equation:

$$r = \frac{\sum XY - \frac{(\sum X)(\sum Y)}{n}}{\sqrt{\left(\sum X^2 - \frac{(\sum X)^2}{n}\right)\left(\sum Y^2 - \frac{(\sum Y)^2}{n}\right)}}$$

$$n = number\ of\ cases$$

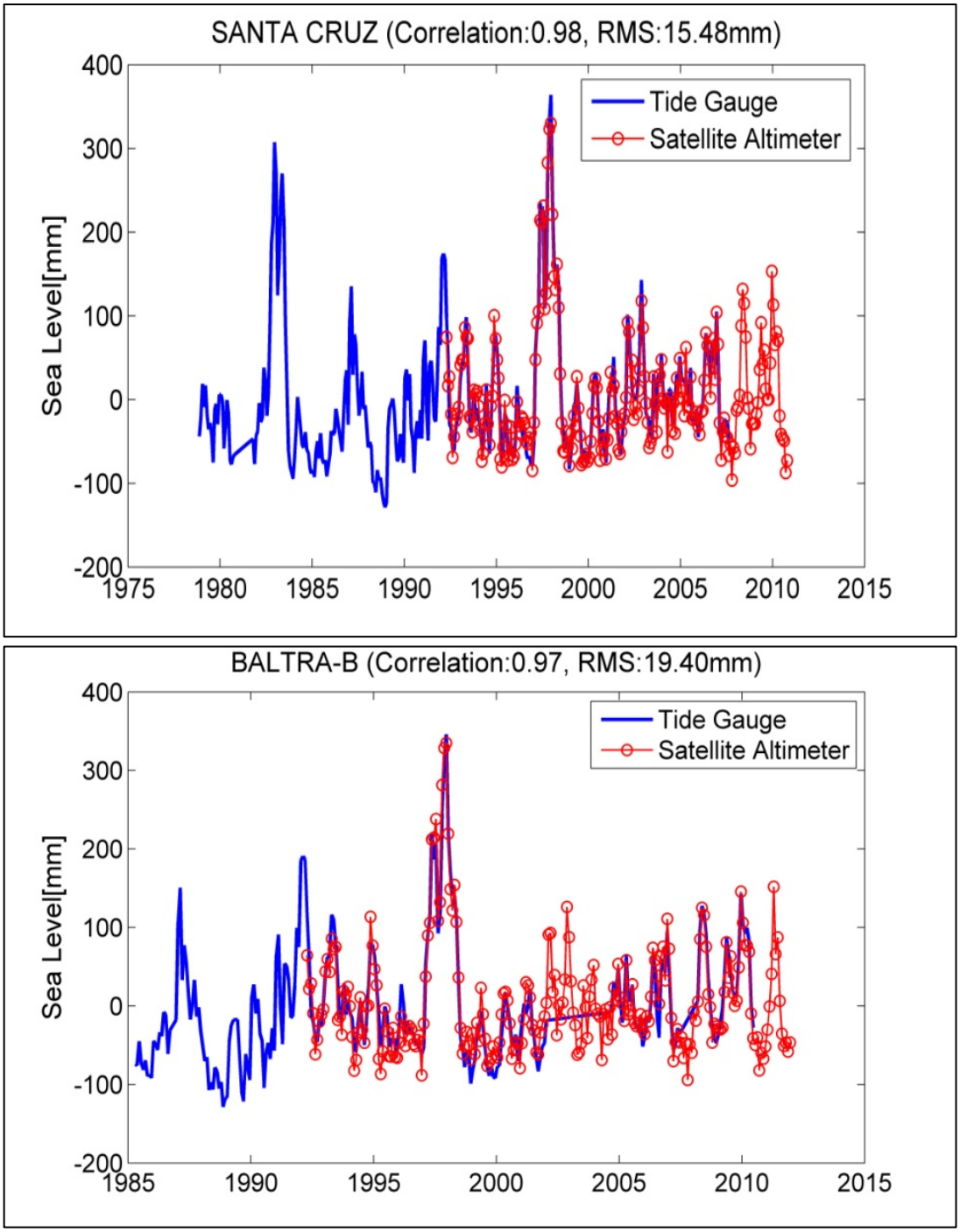

Fig. 2 Plots show a significant correlation and also low RMS value between the TOPEX and Jason-1 MSLA and tide gauge data at two separate tide gauge locations. Spikes in the amplitude of both lines indicate an El Niño event. It is noted that the Santa Cruz tide gauge record shows the 1982 El Niño event, which is not measured by TOPEX as it was launched in 1992, nor by the Baltra tide gauge as its record started in 1985.

Manipulating and Plotting SSTA and MSLA Data

Once I was satisfied with the correlation values, I concluded that the altimeter data had an acceptable accuracy and were a good choice to compare the two El Niño phenomena.

The Satellite altimeter's data were taken for both Sea Surface Temperature (SST) and Sea Surface Height (SSH), or mean sea level (MSL). The raw data for both SST and MSL were supplied by CNES on their Aviso^{+} website. For the creation of the processed plots, sea surface height data were downloaded for both delay mode and near-real time mode from the French's Aviso website [http://www.aviso.altimetry.fr/en/data/products/sea-surface-height-products/global/msla-mean-climatology.html#c10360 & http://www.aviso.altimetry.fr/en/data/products/sea-surface-height-products/global/msla-h.html]. Delay-mode (DM) data are altimetry data that are taken monthly where near-real time (NRT) data are transcribed daily. The daily data (NRT) was averaged and changed into monthly data. This procedure created a bias between the global averaged DM and NRT data within its overlapping period. However, the bias is sufficiently small (0.016 centimeters) and that it was subsequently ignored. Temporal coverage used for the delay-mode MSL data is from January 1993 to December 2014. For near-real time MSL data, the temporal coverage was from January of 2015 to February of 2016.

Next, the annual and semi-annual cycle was removed from both DM and NRT data in order to reduce the noise on the processed plots. The cycles were removed using the following equations:

$$\text{Annual} = A * \cos(2\pi t) + B * \sin(2\pi t)$$

$$\text{Semi-Annual} = C * \cos(4\pi t) + D * \sin(4\pi t)$$

$$a_i = [yr_i \cos(2\pi t * yr_i) \sin(2\pi t * yr_i) \cos(4\pi t * yr_i) \sin(4\pi t * yr_i)]$$

$$N = (a)^T * a, n = (a)^T * SLA, X = \frac{n}{N}$$

A = X(3,1), B = X(4,1), C = X(5,1), D = X(6,1)

i: the i^{th} time, yr_i: time(i)-time(1) [time(1)=1993/01], SLA: the sea level anomaly

De-SLA = SLA- Annual- Semi-annual

This same procedure was executed for the SST data, but the data were downloaded from NOAA [http://www.esrl.noaa.gov/psd/data/gridded/data.noaa.oisst.v2.html]. The newly processed data were added into Excel files and SST and MSL gridded plots showing global features were plotted using Generic Mapping Tools (GMT) software. The plots were divided into 4 groups, SSH or MSL from 1994-1998; 2012-2016 and SST from 1994-1998; 2012-2016. Microsoft Paint© brightened the colors and allowed the title to be changed for each plot. Finally, using Windows Movie Maker©, the plots were compiled into each of their respective groupings and given a duration of one second.

For the longitude time plots, the original data (SST and MSL from) were manipulated using Matlab and the longitude-time data were calculated and averaged over ± 5 degrees latitude bands. That calculation was done using this equation:

$$Mean(long,\ i) = \left[\sum_{lat=-5}^{+5} De - SLA(long, lat, i) \right] / Num$$

i: the i^{th} time, Num: the number of data at each longitude

The corrected data were plotted using software available from Aviso. Seasonal variation was removed from both groups of data. However, the altimetry data for SSH were unavailable from 1982 until 1993 and this lack is reflected in the longitude time plots.

RESULTS

MSLA and SSTA of 1997 and 2015 El Niño Episodes

The cluster of graphs below uses data compiled from the Aviso website as data product of TOPEX/Poseidon, Jason-1, Jason-2, and Envisat satellites that were averaged from readings taken every 10 days. **Fig. 3** shows the evolution of MSLA and SSTA during the 1997/1998 El Niño event, while **Fig. 4** shows the evolution of MSLA and SSTA during the 2015/2016 El Niño. The compilations of plots were selected due to their high intensities during each time. In both figures, all of the plots show the largest intensities (accumulation of red) in the eastern portion of the plot near northern South America and along the equatorial line. It is important to note that the units for MSLA and SSTA are not the same. The scale of MSLA ranges from a decrease in sea level of 30 centimeters (dark blue) to an increase of 30 centimeters (dark red). The scale for SSTA is a much smaller range with a cooling of surface waters by 3°Celcius (dark blue) to an influx of 3°Celcius (dark red) in surface waters. The data were then manipulated to create the two longitude-time plots using longitude-time equation. These two plots compare the sea surface temperature anomaly (SSTA) and mean sea level anomaly (MSLA) covering the two El Niño (also the 1983 El Niño from the SSTA plot), with a longer temporal range (**Figs. 5 & 6**).

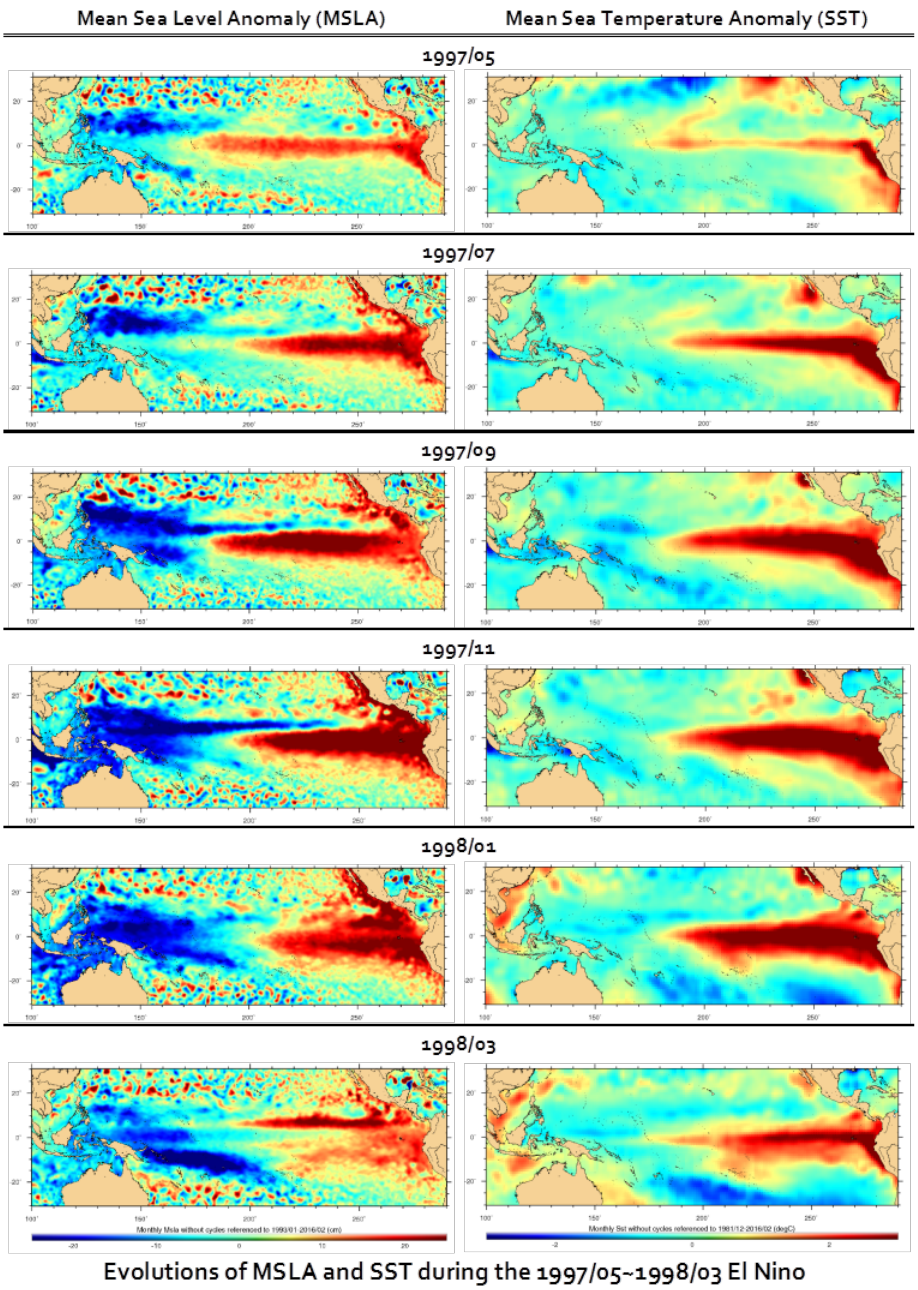

Fig. 3: Evolutions of 1997/1998 El Niño for MSLA and SSTA (left and right panels).

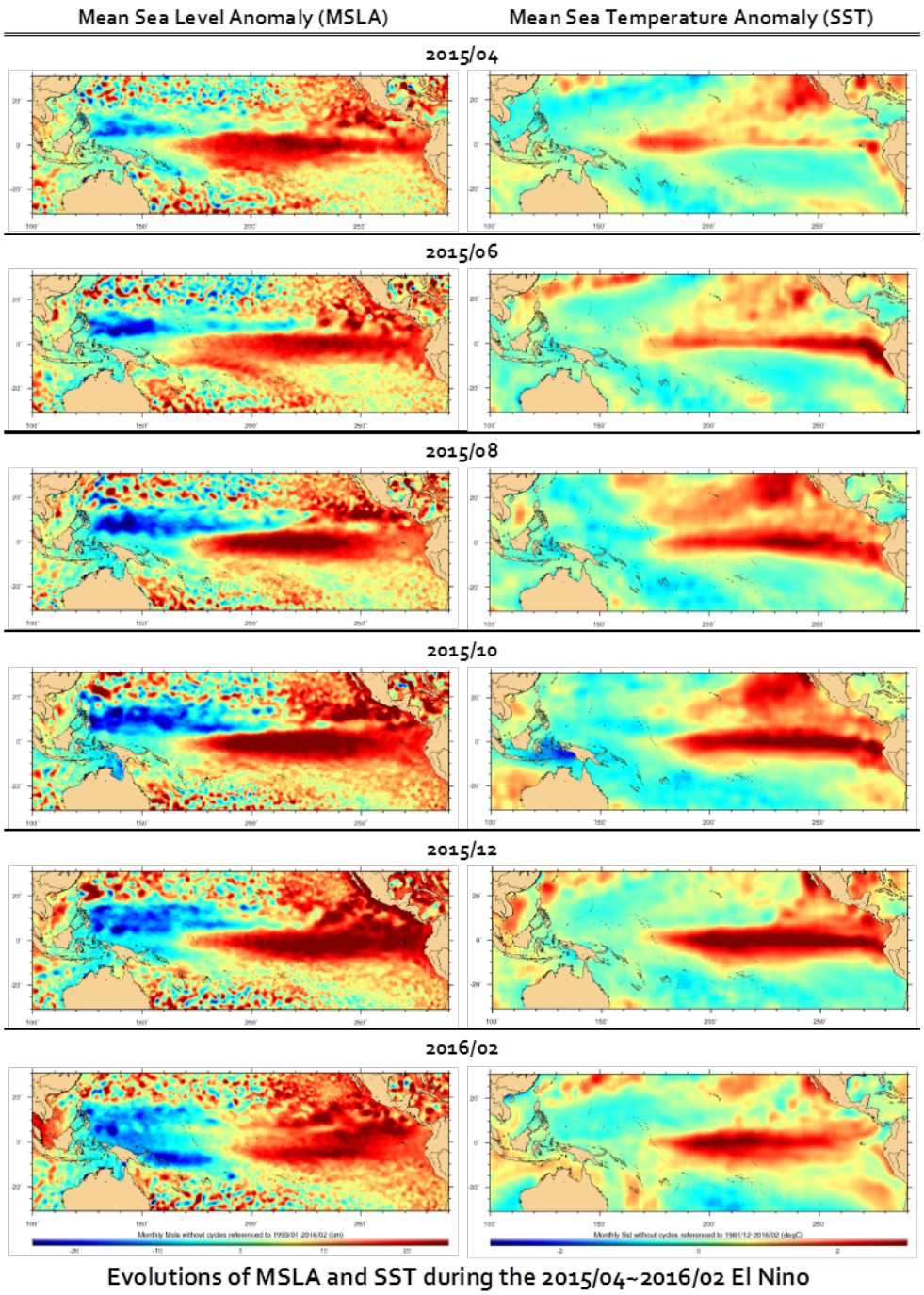

Fig. 4: Evolutions of 2015/2016 El Niño for MSLA and SSTA (left and left panels).

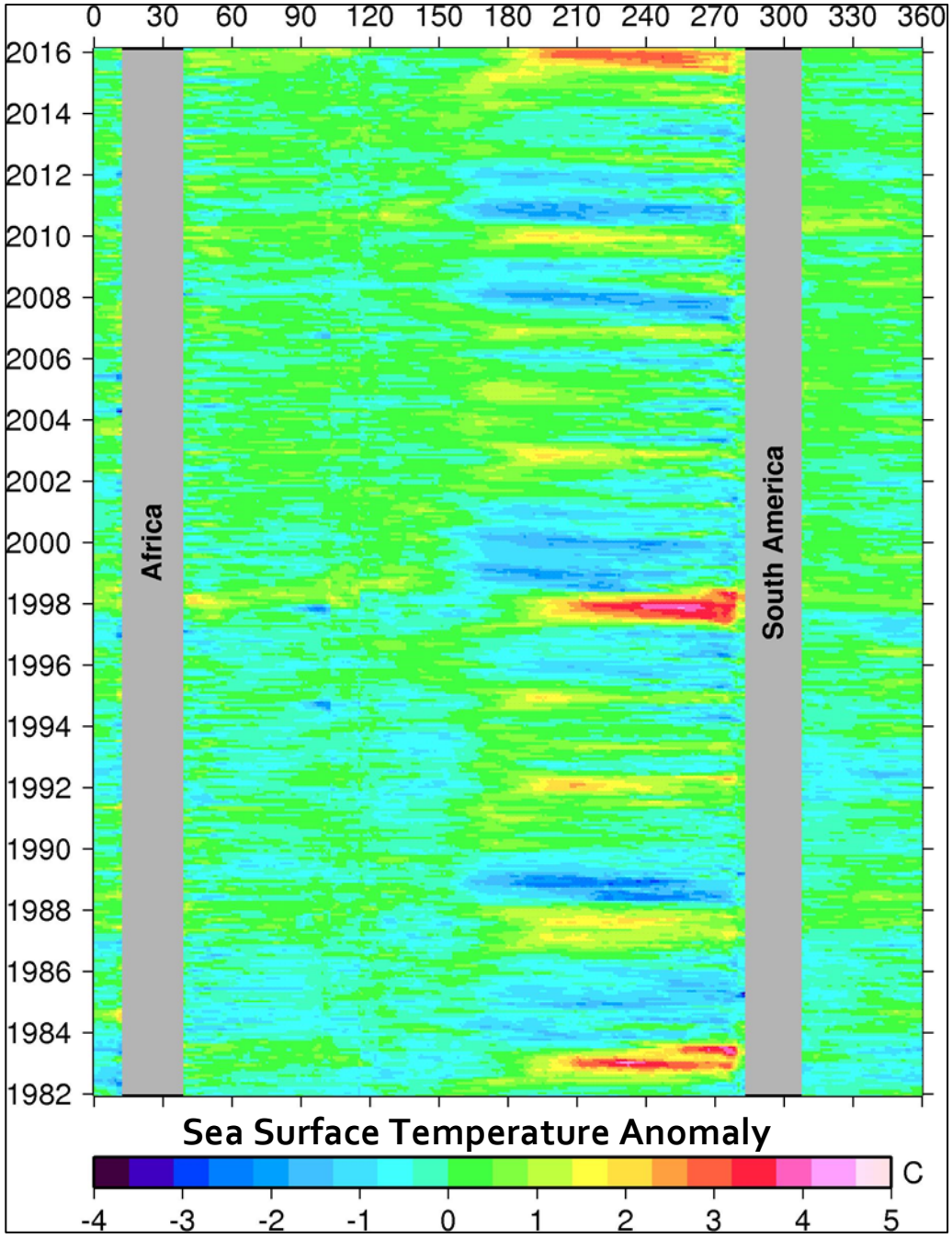

Fig. 5: Longitude Time Plot of Sea Surface Temperature Anomaly (SSTA), 1982–2016. Horizontal axis corresponds to longitudinal axes on the globe. The data are averaged for each longitude point with data between –5 to +5 degrees of latitude. Vertical axis marks the year for each cluster of color. Gray strips indicate land/continents with data outages. The SSTA data are also shown for historic data before 1992, to show the El Niño occurrence during 1982/1983.

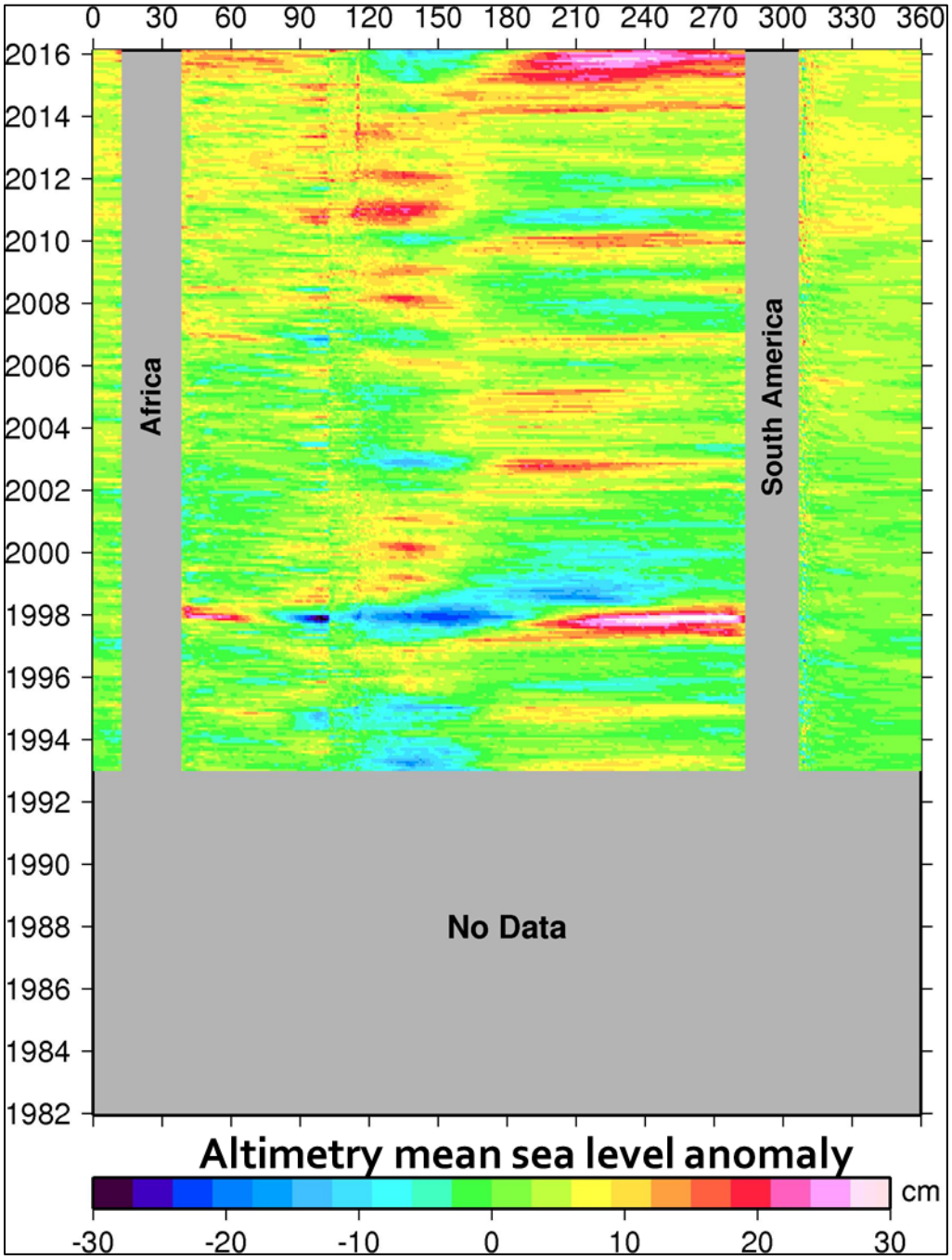

Fig. 6: Longitude Time Plot of Mean Sea Level Anomaly (MSLA). Horizontal axis corresponds to longitudinal axes on the globe. The data are averaged for each longitude point with data between –5 to +5 degrees of latitude. Vertical axis marks the year for each cluster of color. Gray strips indicate land/continents with data outages. Data unavailable prior to 1993 and is labeled as such. Satellite altimeter data starts in 1992 (TOPEX/Poseidon mission). The start at 1982 is to be commensurate with the start time of the SSTA longitude time plot (**Fig. 5**).

Discussion

As mentioned in the earlier literature, I correlated the tide gauge data from two different tide gauge locations in the Galápagos Islands to test the accuracy of the satellite altimeter data: Santa Cruz and Baltra-B (**Fig. 2**). This graph plots both sets of data from the early 1980s (mid 1980s for Figure 7) to the early 2010s. Unfortunately, we do not have tide gauge data at these locations beyond 2008, so the correlation value cannot be added to values from the 2015 El Niño event. Using the statistical analysis, we are looking for the data correlation to be close to 1 in order to suggest accuracy between the two measurement tools.

The Santa Cruz graph has a coefficient value of 0.98 and the Baltra-B graph has a value of 0.97 (**Fig. 2**), respectively, and residual root-mean-square (RMS) values below 20 millimeters for both figures, indicating excellent agreement. The correlation values for the graphs are sufficiently accurate and reiterate how accurate satellite radar altimeters can be from more than 50 kilometers in the atmosphere (Zandbergen et al., 1990). The error within the altimetry data can be attributed to many causes such as the errors in the delay signals and the radial error of the receiving satellite, and other errors such as electromagnetic bias, orbits, and other geophysical or instrument corrections (Zandbergen et al., 1990).

With a Pearson correlation value sufficiently close to 1, I was able to move into the next step of my research. The processed data were plotted along longitudinal and latitudinal axes (for SSH data) during both episodes and depicts the anomaly values of SSH in the Pacific (**Fig. 4 & 5**). The excess of sea water which attributes to the higher sea levels is predominately in the eastern equatorial Pacific region. Conversely, we see a sea surface height decrease in the western equatorial Pacific, a phenomenon that scientists have attributed to a weakening in westward-blowing trade winds along the equator. This weakening is created by pressure changes in two stable air masses over Darwin, Australia and Tahiti (Wyrtki, 1985). With these two pressures and the easterly trade winds

weakened, the ocean current that draws surface water from the coast of South America is reduced. The pressure gradient between these two locations can alter the amount of precipitation that occurs along the equator. The influx of abnormally high amounts of precipitation in the eastern portion of the central Pacific creates higher amounts of water at that location. Moreover, there is a reduction in the amount of upwelling of nutrient-rich, colder waters creating that accumulation of warm water off the coast of South America (**Fig. 4 & 5**). This phenomenon which disturbs cold water upwelling accounts for the warmer sea surface temperatures that clusters around the equatorial Pacific (**Fig. 3 & 4**). These patterns are similar in both hydrodynamic processes suggesting that these temporally separate events both underwent similar processes.

The plots also suggest that the greatest intensities for MSLA and SSTA are the most prevalent during in December of each respective El Niño event. The longitude time plot (**Fig. 5 & 6**) act as another qualitative comparison of El Niño events, however; these plots show the temperature and height anomalies over a larger time span (**Fig. 5)**. There are three distinct times where there was a large increase in the Pacific's ocean temperatures. These times, 1983, 1997, and 2015, all correlate with strong El Niño's of the recent past. Similar patterns are noticeable with the mean sea level anomaly (**Fig. 6**). Conversely, there are some smaller anomalies of sea level during years without a strong El Niño indicator. These plots, also allow for an easier contrast between the two episodes and suggest that the 1997 El Niño event had a larger increase in sea surface temperature than in 2015 (**Fig. 5**). For the sea level data, there too seems to be a higher concentration of water indicated by the lighter colors within, but the 2015 event appears to have a greater spatial reach longitudinally and it appears to have lasted longer temporally (**Fig. 6**). It should be note that 2015/2016 El Niño seems to be still ongoing.

In the same regard, NOAA has been using their network of buoys to monitor the 2015/2016 El Niño event. As of March of 2016, the researchers have found that the largest

anomaly value of the 1997/1998 El Niño event was a 2.5º Celsius increase in the SST during December and November of 1997 (**Fig. 8**). For the 2015/2016 El Niño, that largest value was noticeably smaller at only 2.3º Celsius for just December of 2015 (**Fig. 8**). These values were accrued by NOAA's Ocean Niño Index or ONI. It is important to keep in mind that conditions indicate an El Niño when the ONI is +0.5°C or higher (Dahlman, 2016), and thus this graph includes many more El Niño events than just the two my study focuses on.

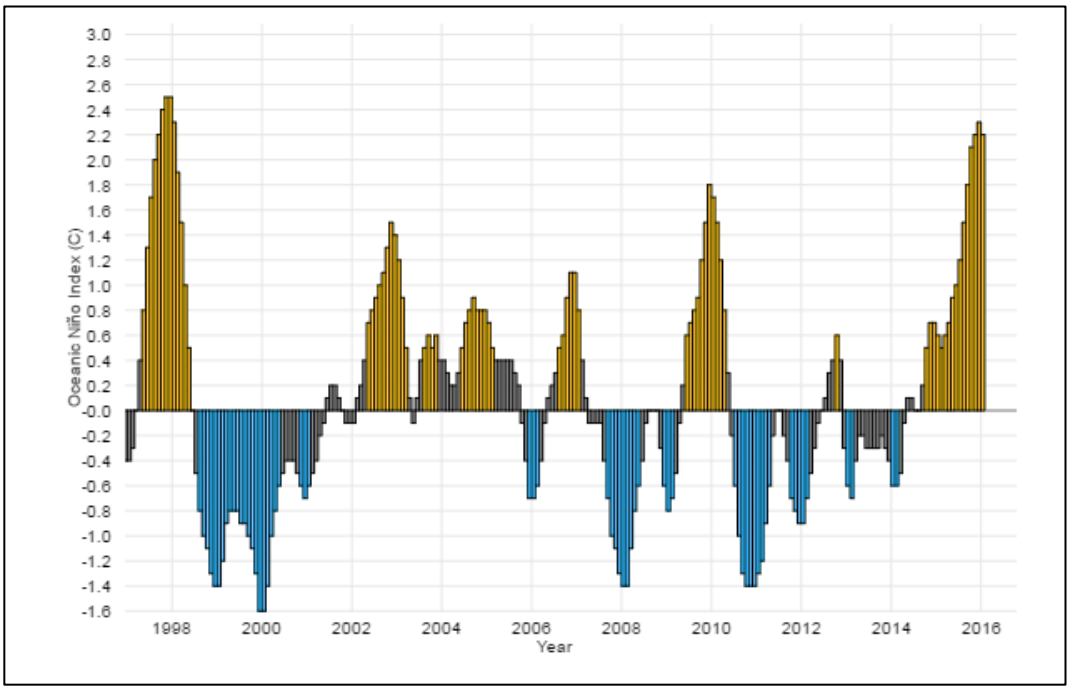

Credit: NOAA

Fig. 7: Oceanic Niño Index (ONI) featuring both El Niño events. NOAA uses a series of buoys for SSTA data.

Using the satellite altimeter data to compare the MSLA and SSTA of the 2015 and 1997 El Niño events, I can conclude that the 1997/1998 El Niño event has a larger and more widespread accumulation of increased sea water in the eastern Pacific and a more intense increase in sea surface temperature than the 2015/2016 El Niño event through February 2016. This suggests that the processes that affected the equatorial Pacific Ocean during both El Niño events (atmospheric forcing and weakening trade winds) were more intense or magnified during 1997. These findings are

consistent with those of the agencies that rely heavily on buoys measurements and calculations, like NOAA, which have directly measured the ocean's ongoing conditions. In contrast, the 2015 El Niño is still going on at the time of the writing of this thesis. These findings are dependent only on data ending in February of 2016, meaning that the interpretation could change in the future. It also cannot be concluded that a more intense buildup of sea water and higher ocean surface temperatures suggests a stronger El Niño episode than another. Atmospheric circulation, weather patterns, and more recently climate change could have a large effect on an El Niño's effects; each of which make it not possible without additional information, to deem one single event as the "Strongest El Niño on Record."

Conclusions

The utilization of satellite altimetry in oceanography is still a young science, but the practicality of satellite altimetry far surpasses its age. When compared to data from *in situ* instruments or tide gauges, the satellite altimeter is highly accurate and also due to its global coverage. With correlation coefficients of 0.98 and 0.97 respectively for two separate locations near the Galápagos Islands in the Eastern Pacific Ocean. The satellite altimetry observed ocean topography and the satellite radiometry observed sea surface temperature data from space allow researchers to use the data to for studying the ocean and the El Niño's.

The computed anomalies to which the time series are referenced, or subtracting a mean value for the time period, make it possible to contrast both El Niño events qualitatively. The comparison of the two events reveal similar patterns where warm surface water builds up in the eastern equatorial Pacific, thus increasing both SSTA and MSLA in that region. However, the longitude time plots reveal a sea surface temperature and sea level anomaly larger in the 1997 El Niño event. This conclusion is tentative, as the 2015 episode is still ongoing as of the end of data analysis period in February of 2016. Furthermore, El Niño, a 'southern oscillation', is constantly interacting with the atmosphere and weather patterns. Its affects could be mitigated by such processes or magnified across the globe. To conclude which event is the strongest would require a more research within that topic.

Recommendations for Future Work

Future work would require an in-depth study conducted over the effects ENSO has on local weather patterns and its subsequent climate. Dependent upon a region's location, El Niño affects all of the continents and islands that surround it. El Niño's adverse effects can differ; causing changes in a nation's precipitation resulting in flooding or droughts, unusually warm winters, and even extreme weather. The extreme weather is triggered by the stationary heat over the Pacific Ocean and re-routes major air currents and creating strong storms (Monastersky, 2016). Locations for this study would be determined and weather records for each would be studied. Seasonal and monthly weather patterns could be analyzed and compared to the El Niño years much in the same way this study was conducted.

Another avenue for research might be to determine how climate change can intensify El Niño conditions in both the Pacific and in the surrounding nations. The data of this study suggested a sea surface height anomaly lasting much longer than previous studies. The increasing CO_2 and warming that follows could be magnifying an El Niño's already wild behaviors (Chavez et al., 1999). To address this question, scientists would need temperature and carbon data from multiple locations. The use of isotopes might be an appropriate choice. Since the analysis of living objects such tree rings, corals, or foraminifera within the ocean's water column would give an accurate reconstruction of the history of the world's temperature gradient via $\delta^{18}O$ isotopes and atmospheric CO_2 via $\delta^{13}C$ isotopes (Ghosh & Brand, 2003). Those analyses could be compared to the Earth's natural ENSO events. It is important to note that foraminifera and tree rings have a temporal resolution too large to be useful for recent El Niño episodes, and only coral cores have an annual resolution (Carriquiry et al., 1994).

REFERENCES CITED

Carriquiry, J.D., Risk, M.J., and Schwarcz, H.P., 1994, Stable isotope geochemistry of corals from Costa Rica as proxy indicator of the EL Niño/southern Oscillation (ENSO): Geochimica et Cosmochimica Acta, v. 58, p. 335–351, doi: 10.1016/0016-7037(94)90468-5.

Chavez, F.P., Strutton, P.G., Friederich, E., Feely, R.A., Feldman, G.C., Foley, D.G., and McPhaden, M.J., 1999, Biological and Chemical Response of the Equatorial Pacific Ocean to the 1997-98 El Niño: Science Magazine , v. 286, p. 2126–2131, doi: 10.1126/science.286.5447.2126.

CNES/CLS, 1997-2014, Aviso+, Monthly Mean and Climatology Maps of Sea Level Anomalies: http://www.aviso.altimetry.fr/en/data/products/sea-surface-height-products/global/msla-mean-climatology.html#c10360 (February 2016).

CNES/CLS, 1997-2014, Aviso+, Maps of Sea Level Anomalies: Height: http://www.aviso.altimetry.fr/en/data/products/sea-surface-height-products/global/msla-h.html (February 2016).

Dahlman, L.A., 2016, Climate Variability: Oceanic Niño Index: Climate.Gov (February 2016)

El Niño: El Niño-Southern Oscillation (ENSO), 2015, National Geographic | Education.

Ghosh, P., and Brand, W.A., 2003, Stable isotope ratio mass spectrometry in global climate change research: International Journal of Mass Spectrometry, v. 228, p. 1–33, doi: 10.1016/s1387-3806(03)00289-6.

Manzello, D.P., Enochs, I.C., Bruckner, A., Renaud, P.G., Kolodziej, G., Budd, D.A., Carlton, R., and Glynn, P.W. 2014. Galapágos Coral Reef Persistence after ENSO warming across an acidification gradient: Geophysical Research Letters, v. 41, p. 9001-9008.

Monastersky, R., 2016, Monster El Niño probed by meteorologists: Nature, v. 529, p. 267–268, doi: 10.1038/529267a.

NOAA: Current Operational SST Anomaly Charts for 2016, 2016, http://www.ospo.noaa.gov/Products/ocean/sst/anomaly (February 2016)

Permanent Service for Mean Sea Level, 2016, Data: http://www.psmsl.org/data/(February 2016)

Troccoli, A., Harrison, M., Anderson, D.L.T., and Mason, S.J., 2008, Seasonal climate: Forecasting and Managing Risk: Dordrecht, Springer.

Wyrtki, K., 1985, Water displacements in the Pacific and the genesis of El Niño cycles: Journal of Geophysical Research, v. 90, p. 7129–7132, doi: 10.1029/jc090ic04p07129.

Ying, J., Huang, P., and Huang, R., 2016, Evaluating the formation mechanisms of the equatorial Pacific SST warming pattern in CMIP5 models: Adv. Atmos. Sci. Advances in Atmospheric Sciences, v. 33, p. 433–441, doi: 10.1007/s00376-015-5184-6.

Zandbergen, R.C.A., Wakker, K.F., and Ambrosius, B.A.C., 1990, Application of satellite altimeter data to orbit error correction and gravity model adjustment: Advances in Space Research, v. 10, p. 249–267, doi: 10.1016/0273-1177(90)90355-4.

APPENDIX A

Matlab Code For Tide Gauge and Altimeter Data Plots (Written by Taylor Allen & Dr. Junkun Wan)

Editor - C:\Users\Taylor\Desktop\Senior Thesis 2016\sample\sample\tgcom.m

ocean_toolbox.m | tgcom.m

```
14      %Read Tide Gauge Data (PSMSL monthly data with IB correction)
15 -    tgdata=load(sprintf('tg/%d.rlrdata',tgID));
16 -    tg_t=tgdata(:,1);
17 -    tg_h=tgdata(:,2)-mean(tgdata(:,2)); %Remove offset
18
19      %Read Altimeter Data (Generated by Junkun Wan from RADS)
20 -    altmat=load(sprintf('alt/%d.mat',tgID));
21 -    alt_t=altmat.multi_alt_mat(:,1);
22 -    alt_h=altmat.multi_alt_mat(:,2);
23
24      %To get altimeter & tg data during overlapping time period for comparison
25 -    k=0;
26 -    for i=1:length(tg_t)
27 -        for j=1:length(alt_t)
28 -            if abs(tg_t(i)-alt_t(j))<1e-3
29 -                k=k+1;
30 -                com_t(k)=tg_t(i);
31 -                com_tg_h(k)=tg_h(i);
32 -                com_alt_h(k)=alt_h(j);
33 -                break;
34 -            end
35 -        end
36 -    end
37
38      %compute correlation
39 -    com_cor_coef=corrcoef(com_tg_h,com_alt_h);
40 -    com_cor=com_cor_coef(1,2)
41
42      %compute RMS
43 -    com_dif=com_alt_h-com_tg_h;
44 -    com_rms=std(com_dif)
45
46
47      %Draw the time series
48 -    plot(tg_t,tg_h,'-b',alt_t,alt_h,'-or')
49 -    xlim([1975,2015])
50 -    ylabel('Sea Level[mm]','fontsize',15)
51 -    legend('Tide Gauge','Satellite Altimeter')
52 -    title(sprintf('%s (Correlation:%4.2f, RMS:%4.2fmm)',tgname,com_cor,com_rms),'fontsize',15)
53 -    set(gca,'fontsize',14)
```